Publications of the Astronomical Society of Australia (PASA), Vol. 35, e025, 8 pages (2018).
© Astronomical Society of Australia 2018; published by Cambridge University Press.
doi:10.1017/pasa.2018.24

A New Globular Cluster in the Area of VVVX

E. Bica[1], D. Minniti[2,3,4], C. Bonatto[1,6] and M. Hempel[5]

[1]Departamento de Astronomia, Universidade Federal do Rio Grande do Sul, Avenida Bento Gonçalves, 9500 – Agronomia, Porto Alegre – RS, 91509-900, Brazil
[2]Instituto Milenio de Astrofisica, Santiago, Chile
[3]Vatican Observatory, V00120 Vatican City State, Italy
[4]Departamento de Fisica, Facultad de Ciencias Exactas, Universidad Andrés Bello, Av. Fernandez Concha 700, Las Condes, Santiago, Chile
[5]Pontificia Universidad Católica de Chile, Instituto de Astrofisica, Av. Vicuña Mackenna 4860, Santiago, Chile
[6]Email: charles@if.ufrgs.br

(Received March 19, 2018; Accepted May 23, 2018)

Abstract

We communicate the discovery of a new globular cluster in the Galaxy that was first detected on WISE/2MASS images and is now confirmed with VVVX photometry. It is a Palomar-like cluster projected at $\ell = 359.15°$, $b = 5.73°$, and may be related to the bulge. We derive an absolute magnitude of $M_V \approx -3.3$, thus being an underluminous globular cluster. Our analyses provide a reddening of $E(B-V) = 1.08 \pm 0.18$ and a distance to the Sun $d_\odot = 6.3 \pm 1$ kpc, which implies a current position in the bulge volume. The estimated metallicity is [Fe/H] $= -1.5 \pm 0.25$. It adds to the recently discovered faint globular cluster (Minniti 22) and candidates found with VVV, building up expectations of ≈50 globular clusters yet to be discovered in the bulge. We also communicate the discovery of an old open cluster in the same VVVX tile as the globular cluster. The VVVX photometry provided $E(B-V) = 0.62 \pm 0.1$, $d_\odot = 7.6 \pm 1$ kpc, and an age of 1.5 ± 0.3 Gyr. With a height from the plane of ≈0.8 kpc, it adds to nine Gyr-class clusters recently discovered within $0.8 \leqslant Z \leqslant 2.2$ kpc, as recently probed in the single VVV tile b201. We suggest that these findings may be disclosing the thick disk at the bulge, which so far has no open cluster counterpart, and hardly any individual star. Thus, the VVV and VVVX surveys are opening new windows for follow-up studies, to employ present and future generations of large aperture telescopes.

Keywords: (Galaxy:) globular clusters: general – (Galaxy:) open clusters and associations: general

1 INTRODUCTION

Globular clusters (GCs) are fossils that allow one to retrieve information about the formation phase of galaxies and their early evolution (e.g. Minniti 1996, Côté 1999, Brodie & Strader 2006, Ortolani et al. 2011). Any new GC detected is welcome to improve the statistics of parameters such as metallicity and position distributions in the bulge and halo subsystems (Bica, Ortolani, & Barbuy, 2016). Some inner bulge GCs might be dynamically trapped in the bar (Rossi et al. 2015).

The ESO–VVV survey is becoming a fundamental tool to put to the test previous scenarios for the bulge formation, and open doors to new ideas and constraints on the GC populations in the Milky Way. Minniti et al. (2017b) showed that VVV photometry settled the GC nature of FSR 1716 (Froebrich, Scholz, & Raftery, 2007). This was achieved by means of analyses of RR Lyrae and colour–magnitude diagrams (CMDs). Harris (2010) compiled 157 GCs in the Galaxy and, by decontaminating halo intruders, Bica et al. (2016) compiled 43 bona fide GCs in the bulge. These numbers are expected to increase in the near future. More recently, Minniti et al. (2017c) discovered a GC and many candidates in the bulge with VVV, which as rule are fainter, looser, less populated, and crowded in dense central bulge and disk fields, as compared to classical GCs. The current census of GCs in the Milky Way is now close to 200, and new estimates for missing ones, especially based on the recent VVV and halo surveys such as the Dark Energy Survey (DES) (e.g. Luque et al. 2017) can amount to 100 undetected GCs. About half of them might still be lurking in the bulge (Minniti et al. 2017c).

VVV contributions are also producing new constraints and insights on the old central disk that permeates and possibly embraces the bulge. Recently, Ivanov et al. (2017) deep-stacked images of a single edge VVV tile, and detected 9-Gyr-old open clusters (OCs). Their heights above the plane are about 1 kpc, and their total number can be speculated to be hundreds or more, considering all the VVV and VVVX tiles.

The present work communicates the discoveries of a GC and an old OC that are new pieces of evidence that help

https://doi.org/10.1017/pasa.2018.24 Published online by Cambridge University Press

Figure 1. VVVX image (JHK_s RGB composition) of the new GC Cmg 1102. Size 5 arcmin × 5 arcmin. East to the left, north to the top.

Figure 2. Same as Figure 1 for the new OC Bc 7. The bright star near the centre is a foreground K star.

better understand the bulge and central disk subsystems in the Galaxy. In Section 2, we present the VVVX observations and the analysis methods. In Section 3, we analyse the new GC, and in Section 4, the new OC. Finally, in Section 5, we provide discussions and concluding remarks.

2 TARGETS, OBSERVATIONS, AND METHODS

The new GC is located at the Galactic coordinates $\ell = 359.15°$, $b = 5.73°$, and equatorial ones $\alpha = 17^h21^m45^s$, $\delta = -26°32'41''$. It is projected near the edge of the central bulge (Barbuy, Bica, & Ortolani 1998) and well within the extended bulge (Bica et al. 2016). We suggest the use of Camargo 1102 (Cmg 1102 for short) as designation. It is important to emphasise the efforts and circumstances that led to the present findings. Cmg 1102, was discovered in a survey of WISE and 2MASS images along the Milky Way disk that provided 1 089 clusters and candidates in two lists (Camargo, Bica, & Bonatto, 2016a). Most are embedded clusters (ECs). Some of these entries and later additions are ECs at relatively high Galactic latitudes, and revealed for the first time star formation in halo clouds (Camargo et al. 2016a; Camargo, Bica, & Bonatto 2016b). All together, these studies amount to 1 101 objects. Cmg 1102 was first analysed with 2MASS photometry that suggested a GC. Finally, the deep near-IR images provided by the VVVX in the present work were necessary to settle the GC nature.

In Figure 1, we show a VVVX J, H, and K_s Red Green Blue (RGB) composite image of Cmg 1102. It is a prominent cluster, however not as a classical populous GC. It can be seen in the optical (DSS). Cmg 1102 resembles the faint GCs detected on Palomar plates, first listed more than half a century ago (Abell 1955; Kinman & Rosino 1962).

The new old OC is projected towards $\ell = 359.50°$, $b = 5.80°$, or $\alpha = 17^h22^m22^s$ and $\delta = -26°12'52''$. We suggest the use of Bica 7 as the cluster designation (Bc 7 for conciseness). Bica 1 through 6 are previous OC findings (e.g. Bica, Bonatto, & Dutra 2003), so designated in DAML02 (Dias et al. 2014). Bc 7 is part of a 20-yr survey of clusters and candidates mostly carried out on DSS, 2MASS, and WISE images by one of us (E.B.). The resulting survey (with more than 10 000 entries), together with a general cluster and candidate catalogue that is deep, updated, cross-identified, and with chronologically ordered designations. This general catalogue ensures that the two present clusters are discoveries, will be soon available. We show in Figure 2 a VVVX J, H, and K_s RGB composite image of Bc 7, where the bright star is HD 157094, a foreground K0V star according to SIMBAD.

2.1. VVVX data

We employ Cambridge Astronomical Survey Unit (CASU) photometry from the VVVX extended survey. The CASU photometry is currently the standard calibration, which is readily available and suitable for our work. We note that there has not yet been PSF photometry made for VVVX fields. This is an on-going work, that requires a much longer time because VVVX is a massive dataset.

Both clusters in the present study are located in tile b0463, at the northern boundary of the VVV survey, in terms of Galactic coordinates. The data were acquired with the VIRCAM camera at the VISTA 4-m telescope at the ESO Paranal

https://doi.org/10.1017/pasa.2018.24 Published online by Cambridge University Press

Observatory. Likewise previous data, they were reduced at the CASU with the VIRCAM pipeline. The observations, calibrations, and photometry follow the standard VVV procedure (see Saito et al. 2012; Minniti et al. 2017b, and references therein).

2.2. Analysis methods

We analysed CMDs and cluster structure in order to establish the two objects as star clusters and their nature, by determining astrophysical parameters. We use the VVVX J (1.253 μm), H (1.662 μm) and K_s (2.159 μm) bands with magnitudes and errors, along with their positions. Below, we briefly describe the employed methods written by one of us (C.B.). With respect to the previous routines applied to many OCs, OCs, and ECs (e.g. Bonatto & Bica 2010), now C.B. developed automated isochrone fits. More details are in Oliveira, Bica, & Bonatto (2018).

To reveal the intrinsic morphology of the CMDs, we employ the algorithm for statistical field-star decontamination in Bonatto & Bica (2007) to the input photometry. It has been widely used (e.g. Camargo et al. 2016a, 2016b) in the study of star clusters of all ages, and sitting on a wide range of background densities. In summary, the routine builds Hess diagrams both for the target region and field stars. The intrinsic Hess diagram corresponds to the subtraction of the latter two.

The astrophysical parameters are derived from the decontaminated photometry following the methods in Lima et al. (2014) (and references therein). We now use the upgraded PARSEC (Bressan et al. 2012) isochrone database convolved to the VVV bands. The output parameters are the total cluster mass $M_{\rm tot}$ (with a mass extrapolation to low mass member stars), age, apparent, and absolute distance moduli, as well as the colour excess $E(B-V)$. Throughout the new analyses, we work with the Hess representation of the observed and theoretical CMDs, to compare them.

A star cluster structure can be represented by its stellar radial density profile (RDP). It is applied in what we call a colour-magnitude filter in the CMD, to isolate the stars with high probability of being cluster members. It creates an intrinsic stellar RDP and enhances its contrast relative to the background. The RDP is constructed from star counts in concentric rings, divided by the corresponding area, providing the surface stellar density. In the present study, we use the single-band Gaia catalogue (Gaia Collaboration et al. 2016) for its depth and resolution.

3 THE NEW GC CMG 1102 IN THE VVVX TILE B0463

The present clusters are very contaminated by their dense fields. Thus, here we use Gaia photometry (G band, $\lambda_{\rm eff}$ = 6418.68 AA, $\omega_{\rm eff}$ = 3 580 AA) to build the RDP because it minimises crowding effects. We present in Figure 3, Gaia RDPs of Cmg 1102, including those for magnitude cutoffs for G < 18, G < 16, and G < 14. Clearly, when brighter stars are

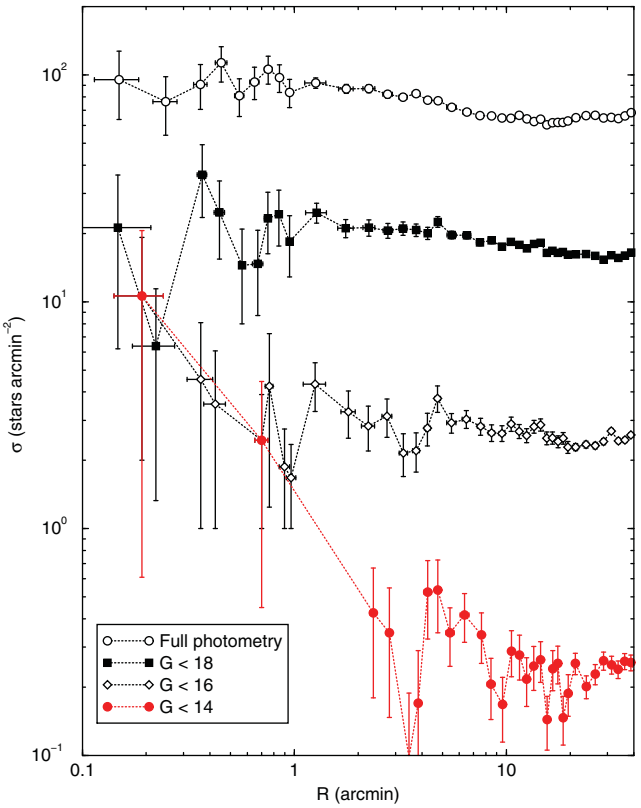

Figure 3. Cmg 1102: RDPs built with Gaia G filter photometry with different thresholds (see inset).

considered, the RDP shows an overdensity ($R \leqslant 2$ arcmin) with increasing contrast with respect to the background. Considering fluctuations, the overdensity may reach an extension of ∼5 arcmin from the cluster centre. This profile guided our cluster extractions for the CMD constructions.

Figure 4 illustrates the decontamination procedure. The total extracted field CMD is subtracted of an equal area outer field, generating the cluster intrinsic sequences.

Figure 5 shows the best isochrone fit (Section 2.2) to the decontaminated CMD of Cmg 1102. This fit leads to an age of ≈13.5 Gyr, the reddening value $E(B-V) = 1.05 \pm 0.30$, a metallicity of $Z \approx 0.03\,Z_{\odot}$ ([Fe/H] ≈ −1.5 for a solar [α/Fe]) and a distance from the Sun $d_{\odot} \approx 6.4 \pm 0.4$ kpc. The total stellar mass (assuming a Kroupa mass function extrapolation to stars of mass $0.1\,M_{\odot}$) results in $\approx 6\,800\,M_{\odot}$ and an absolute V magnitude $M_V \approx -3.3$. Given the photometric depth of VVVX, the observed mass in the CMD amounts to just $\approx 200\,M_{\odot}$, but these are the main contributors to the cluster light. However, we note that dynamical effects may have depleted the primordial stellar mass. Thus, our estimate is an upper limit.

We also compare the decontaminated CMD with mean loci of the nearby GCs M 4 ([Fe/H] = −1.16) and NGC 6397 ([Fe/H] = −2.02) built with 2MASS photometry. The metallicities are from Harris (2010). We obtained these mean loci from their 2MASS CMDs, which are not saturated and reach

https://doi.org/10.1017/pasa.2018.24 Published online by Cambridge University Press

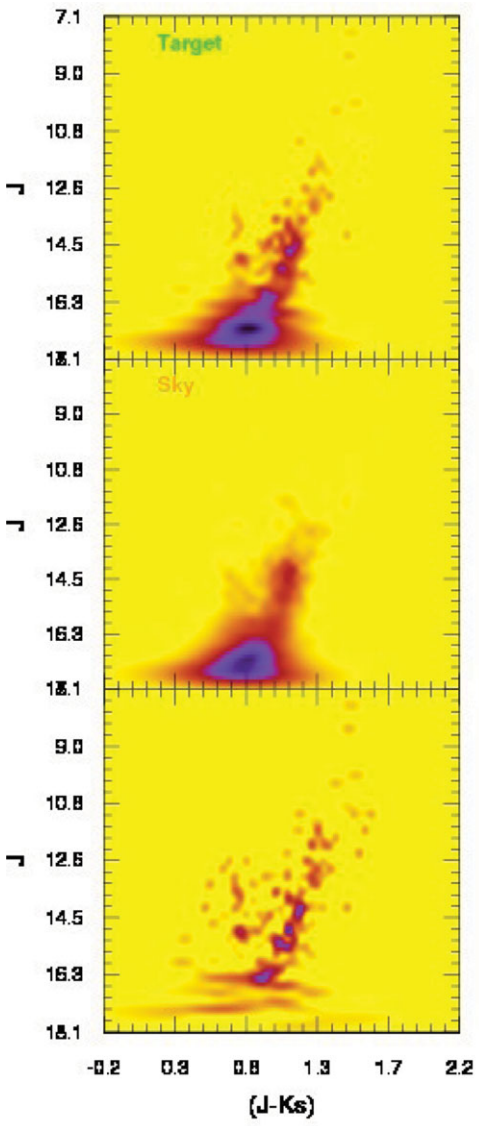

Figure 4. Cmg 1102: Field-star decontamination. Top: all stars within 2 arcmin; middle: field-stars sampled outside the cluster; bottom: decontaminated CMD.

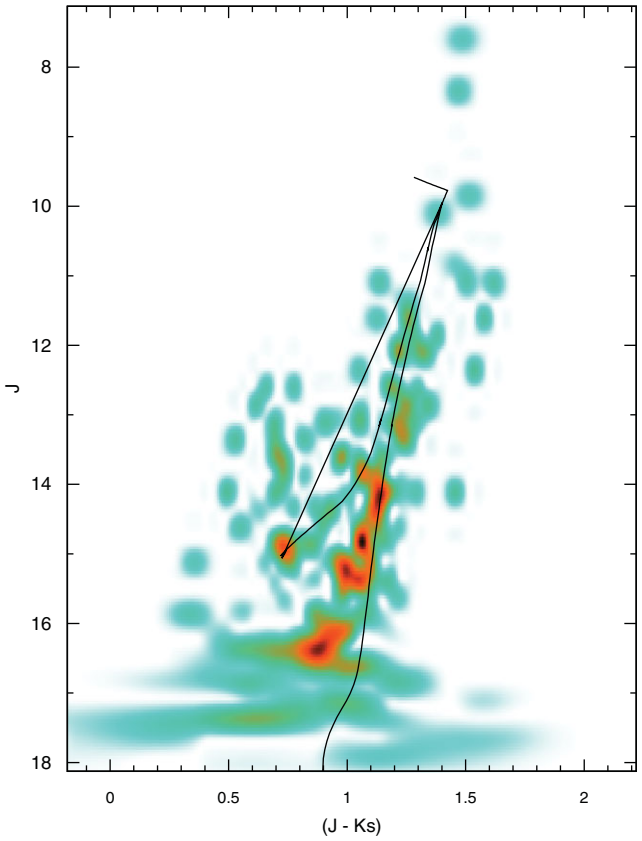

Figure 5. Cmg 1102: Isochrone fit to the decontaminated CMD. The best result corresponds to Age = 13.5 Gyr, $Z = 0.03\,Z_{\odot}$, $d_{\odot} = 6.3$ kpc, and $M = 3.7 \times 10^3\,M_{\odot}$.

faint sequences overlapping the VVV data. The horizontal branch morphology is consistent with the derived metallicity. The superposition of the mean loci (Figure 6) suggest a red HB component at $J \approx 14$, and the possibility of a blue HB component. The mean-loci solutions imply a distance from the Sun within 6.1–7.0 kpc, in good agreement with the isochrone fit result. Given the low content of bright giants, and the possible differential reddening effects, we conclude that its metallicity is compatible with [Fe/H] $\approx -1.5 \pm 0.25$, this within the range between NGC 6397 and M 4. This value and uncertainty would imply either a halo intruder in the Bulge or an intrinsic metal-poor Bulge GC (Bica et al. 2016).

We show in Figure 7 proper motions (from Gaia DR2—Gaia Collaboration, 2018) for the Cmg 1102 and the comparison field. For consistency with the RDP shown in Figure 3, the analysis is limited to stars brighter than $G = 14$. Although the number of member stars is low, there appears to be a more restricted distribution. Cmg 1102 is probably dissolving into the field (e.g. Minniti et al. 2017c).

The derived Galactocentric coordinates are $X_{GC} = -1.04$ kpc, $Y_{GC} = -0.10$ kpc, and $Z_{GC} = 0.70$ kpc, (adopting $X_{\odot} = -8.0$ kpc). At $\ell = 359.15°$, this GC seems to soar above the Galactic centre at a height of ≈700 pc, in the bulge volume.

With $M_V \approx -3.3$, Cmg 1102 is fainter than typical bulge Palomar clusters like Pal 6 ($M_V \approx -6.79$, Pal 7 (IC 1276) −6.67, Pal 8 −5.51, Pal 9 (NGC 6717)-5.56, and Pal 11 −6.92, and comparable to the low-mass GC AL 3 (Harris 2010). On the other hand, Cmg 1102 is more luminous than the faint halo clusters (Luque et al. 2017 and references therein).

One interesting possibility is, in the case of being a bulge member, Cmg 1102 should be an example of a new class of low-luminosity GCs in that component. Such faint candidates—probably the remains of larger clusters that are being evaporated or disrupted in the bulge are being disclosed (e.g. Minniti et al. 2017a, 2017b, 2017c).

https://doi.org/10.1017/pasa.2018.24 Published online by Cambridge University Press

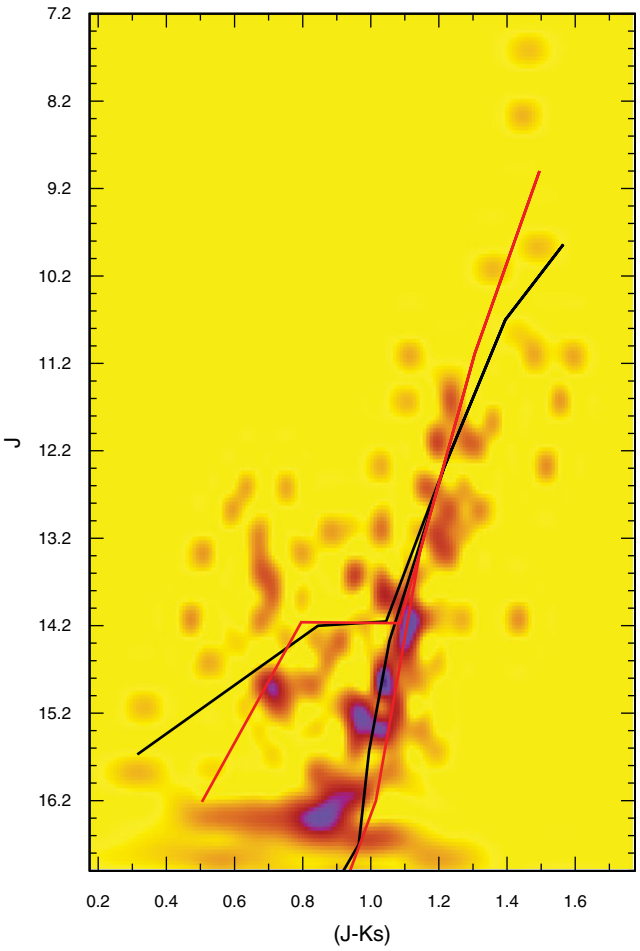

Figure 6. Cmg 1102: Mean-locus of the GCs NGC 6397 ([Fe/H] = −2.02) and M 4 ([Fe/H] = −1.16) superimposed on the decontaminated CMD. For NGC 6397, we applied $\Delta E(J-K_S) = +0.52$ and $\Delta (m-M)_J = +3.0$, resulting in $d_\odot = 6.1$ kpc. For M 4, the values are $\Delta E(J-K_S) = +0.27$ and $\Delta (m-M)_J = +3.0$, resulting in $d_\odot = 7$ kpc.

We note that the GC NGC 6355 is located ≈12 arcmin northwards of Cmg 1102. Unlike Cmg 1102, NGC 6355 has a significant PM difference with respect to the bulge/central disk (Figure 8). The results imply that the two clusters are not kinematically related.

4 THE NEW OLD OC BC 7 IN THE SAME VVVX TILE B0463

We show in Figure 9 the RDP of Bc 7, which shows an excess with observed radial extent of $R \approx 2$ arcmin.

Near the centre of Bc 7 is projected the bright near infrared star HD 157094 (HIP 84996), with $J = 5.156$, $J-H = 0.908$ and $J - K_s = 0.990$, as given in SIMBAD. In the optical, it is also quite bright ($V = 8.09$) which explains why this relatively bright cluster has been so far overlooked. This is a similar case to the Siriusly cluster that was found with Gaia, having been hidden in most previous searches by the Sirius glare (Koposov, Belokurov, & Torrealba 2017).

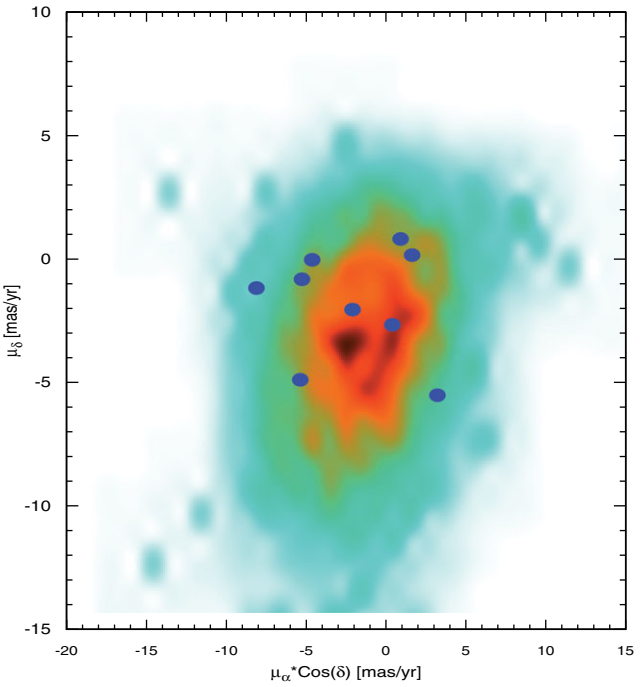

Figure 7. Cmg 1102: Gaia DR2 proper motions. The Hess map shows the PM distribution of the surrounding sky (20 arcmin − 30 arcmin). Blue symbols are for the stars within 3 arcmin.

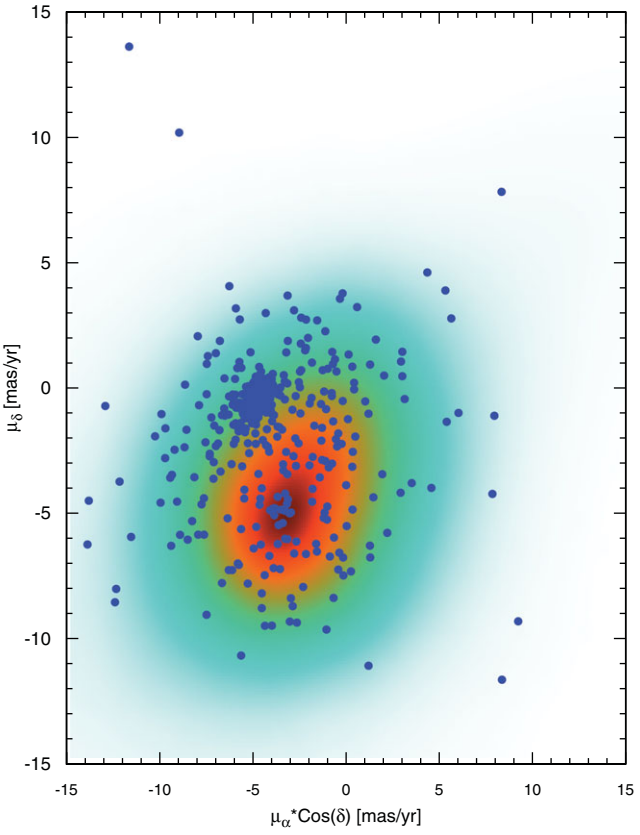

Figure 8. Same as Figure 7 but for the nearby projected GC NGC 6355.

PASA, 35, e025 (2018)
doi:10.1017/pasa.2018.24

https://doi.org/10.1017/pasa.2018.24 Published online by Cambridge University Press

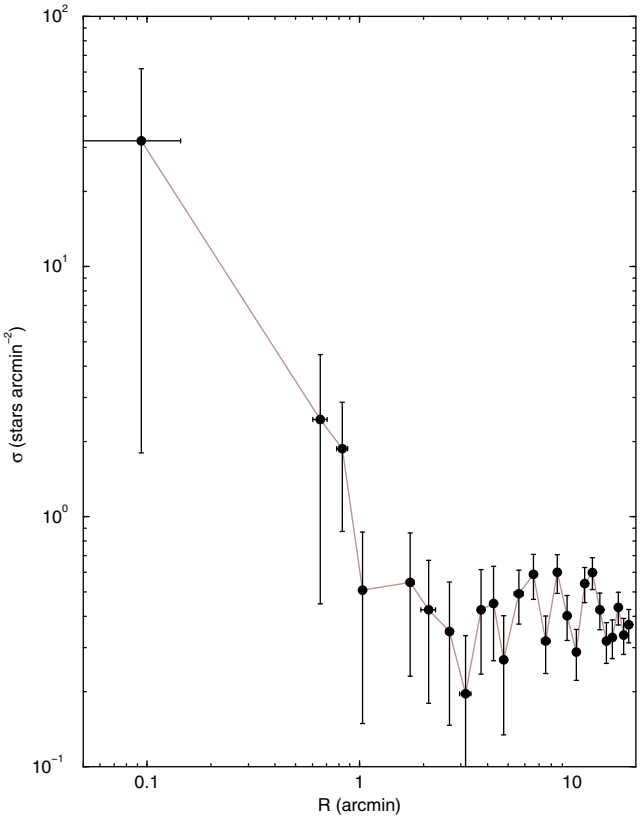

Figure 9. Same as Figure 3 for Bc 7. We employ the constraint $G < 14$ for the Gaia photometry that best describes the cluster stellar distribution.

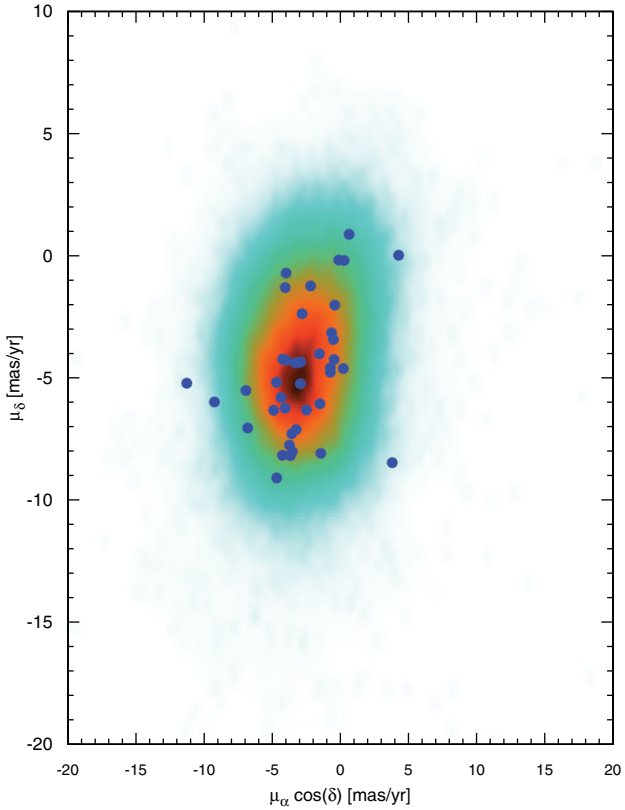

Figure 10. Same as Figure 7 for Bc 7, but for stars with $G < 17$. Cluster stars are extracted within 1 arcmin.

The field-star decontamination for Bc 7 is illustrated in Figure 11, where the intrinsic sequences suggest an old OC.

In order to shed light on this issue, we show the Gaia DR2 proper motions for Bc 7 and comparison field in Figure 10. HD 157094 is a high PM star (SIMBAD) that is outside the cluster/field distribution and an outlier with respect to the field, which confirms that it is a foreground star. Bc 7 has PMs similar to the field, thus possibly co-moving.

In Figure 12, we superimpose the isochrone solution (Section 2.2) on the intrinsic cluster CMD. The turnoff is barely attained, but the RGB, including some SGB and Clump stars constrained the solution. We obtained the following parameters: age ≈1.5 Gyr, reddening $E(B-V) \approx 0.6 \pm 0.1$, distance from the Sun ≈7.6 ± 1.0 kpc, $Z/Z_\odot \approx 1.4 \pm 0.4$ ([Fe/H] ≈ 0.13, for Solar alpha ratios). Finally, the total stellar mass is ≈2 500 $M_\odot$, the observed mass is ≈470 $M_\odot$, and $M_V \approx -4.0$.

5 DISCUSSION AND CONCLUDING REMARKS

We communicate the discovery of a new GC in the Galaxy, and a new old OC as well. These objects were first detected in WISE and 2MASS images, while VVVX photometry in the tile b0463 settled their natures.

Both appear to be new pieces of evidence of a more detailed perspective of the bulge and central disk. Ivanov et al. (2017), with deep-stacked images of the VVV tile b201, found nine old OCs nearly in front and behind the Galactic centre with heights from the plane of about 1 kpc. This fact, together with the present cluster Bc 7 with a resulting height of ≈0.8 kpc, may suggest the first detection of thick disk clusters about the bulge. Deep follow-up studies are necessary to further test this scenario.

Bica et al. (2016) derived a bulge population of 43 GCs, by decontaminating halo intruders. They further indicated 10 candidates from previous VVV lists. More recently, many faint GC candidates were disclosed by Minniti et al. (2017c) in the bulge with VVV. Minniti et al. (2017a) count nearly 200 GCs and candidates in the Galaxy. They further estimate about 100 more yet to be discovered, half of them in the bulge. A new picture of the bulge and the old central disk is emerging. The new GCs can alleviate the specific GC frequency deficit of the Milky Way with respect to M31 (van den Bergh 2010), which persists to date, with M 31 having 361 GCs (Caldwell & Romanowsky 2016). VVV is presently having a major impact on the Galactic GC census, as VVVX also certainly will, from the present results. We emphasise the need of larger telescopes of the present and future generations for follow-up studies.

https://doi.org/10.1017/pasa.2018.24 Published online by Cambridge University Press

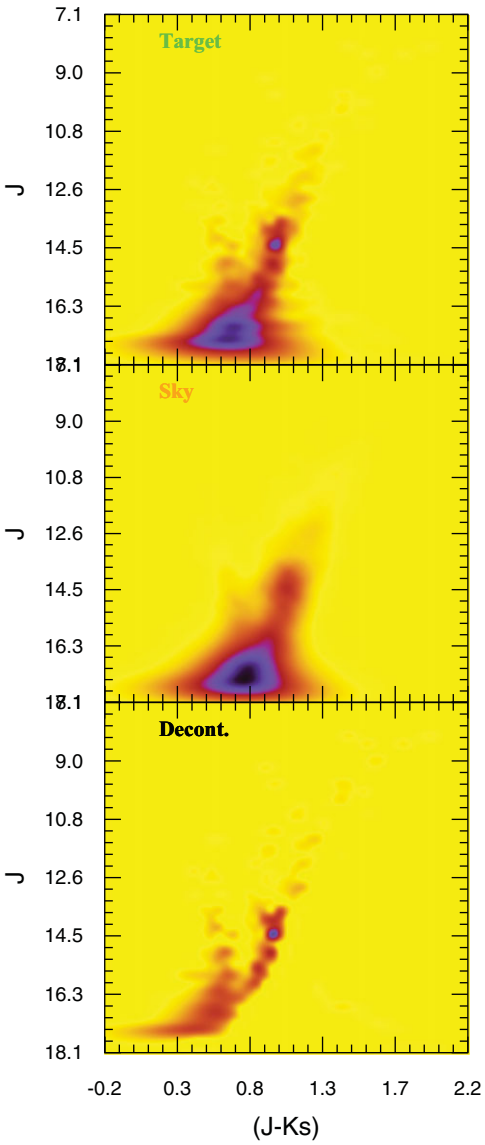

Figure 11. Same as Figure 4 for Bc 7.

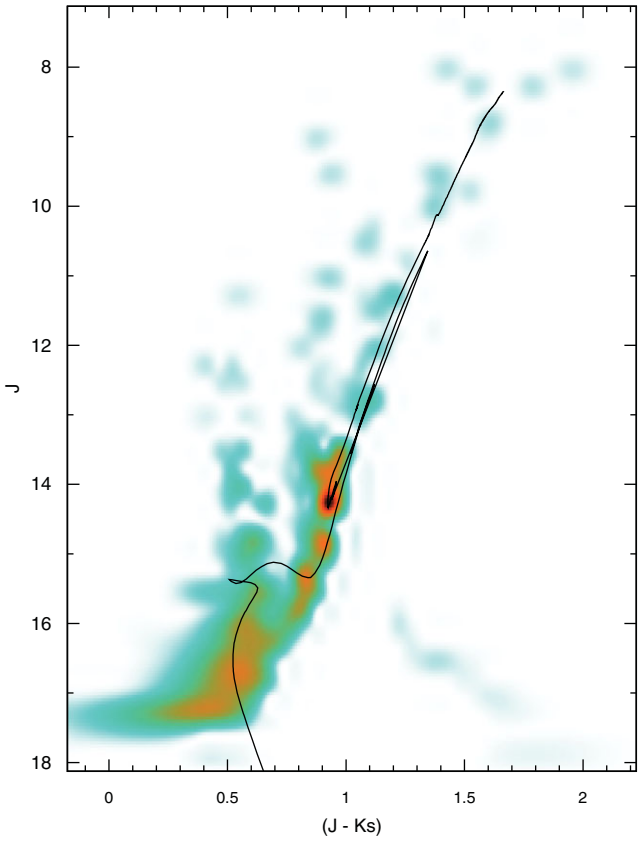

Figure 12. Bc 7: Isochrone fit to the decontaminated CMD.

ACKNOWLEDGEMENTS

We thank an anonymous referee for important comments and suggestions. We thank Dr D. Camargo for communicating us the coordinates of the GC candidate. We acknowledge data from the ESO Public Survey program ID 179.B-2002 taken with the VISTA telescope, and products from the Cambridge Astronomical Survey Unit (CASU). Support for this work was provided by the BASAL Center for Astrophysics and Associated Technologies (CATA) through grant PFB-06, and by the Ministry for the Economy, Development and Tourism, Programa Iniciativa Cientifica Milenio grant IC120009, awarded to the Millennium Institute of Astrophysics (MAS). D. M. acknowledges support from FONDECYT Regular grant No. 1170121. M. H. also acknowledges support from BASAL CATA through grant PFB-06. C.B. and E.B. also acknowledge support from CNPq/Brazil. This research is based on observations collected at the European Organisation from Astronomical Research in the Southern Hemisphere under ESO programs.

REFERENCES

Abell, G. O. 1955, PASP, 67, 258
Barbuy, B., Bica, E., & Ortolani, S. 1998, A&A, 333, 117
Bica, E., Bonatto, C., & Dutra, C. M. 2003, A&A, 405, 991
Bica, E., Ortolani, S., & Barbuy, B. 2016, PASA, 33, e028
Bonatto, C., & Bica, E. 2007, MNRAS, 377, 1301
Bonatto, C., & Bica, E. 2010, MNRAS, 407, 1728
Bressan, A., Marigo, P., Girardi, L., Salasnich, B., Dal Cero, C., Rubele, S., & Nanni, A. 2012, MNRAS, 427, 127
Brodie, J. P., & Strader, J. 2006, ARA&A, 44, 193
Caldwell, N., & Romanowsky, A. J. 2016, ApJ, 824, 42
Camargo, D., Bica, E., & Bonatto, C. 2016a, MNRAS, 455, 3126
Camargo, D., Bica, E., & Bonatto, C. 2016b, A&A, 593, A95
Côté, P. 1999, AJ, 118, 406
Dias, W. S., Alessi, B. S., Moitinho, A., & Lepine, J. R. D. 2014, VizieR Online Data Catalog, 1
Froebrich, D., Scholz, A., & Raftery, C. L. 2007, MNRAS, 374, 399
Gaia Collaboration et al. 2016, A&A, 595, A2
Harris, W. E. 2010, preprint (arXiv:1012.3224)
Ivanov, V. D., Piatti, A. E., Beamín, J.-C., Minniti, D., Borissova, J., Kurtev, R., Hempel, M., & Saito, R. K. 2017, A&A, 600, A112
Kinman, T. D., & Rosino, L. 1962, PASP, 74, 499
Koposov, S. E., Belokurov, V., & Torrealba, G. 2017, MNRAS, 470, 2702
Lima, E. F., Bica, E., Bonatto, C., & Saito, R. K. 2014, A&A, 568, A16
Luque, E., et al. 2017, MNRAS, 468, 97
Minniti, D. 1996, ApJ, 459, 175

https://doi.org/10.1017/pasa.2018.24 Published online by Cambridge University Press

Minniti, D., Alonso-García, J., Braga, V., Contreras Ramos, R., Hempel, M., Palma, T., Pullen, J., & Saito, R. K. 2017a, RNAAS, 1, 16
Minniti, D., et al. 2017b, ApJ, 838, L14
Minniti, D., et al. 2017c, ApJ, 849, L24
Oliveira, P. R. A., Bica, E., & Bonatto, C. 2018, MNRAS, 476, 842
Ortolani, S., Barbuy, B., Momany, Y., Saviane, I., Bica, E., Jilkova, L., Salerno, G. M., & Jungwiert, B. 2011, ApJ, 737, 31
Rossi, L. J., Ortolani, S., Barbuy, B., Bica, E., & Bonfanti, A. 2015, MNRAS, 450, 3270
Saito, R. K., et al. 2012, A&A, 537, A107
van den Bergh, S. 2010, AJ, 140, 1043

https://doi.org/10.1017/pasa.2018.24 Published online by Cambridge University Press